



4th IASPEI / IAEE International Symposium:

Effects of Surface Geology on Seismic Motion

August 23–26, 2011 • University of California Santa Barbara

COUPLED TOPOGRAPHY-STRATIGRAPHY EFFECTS DURING THE M7.0 HAITI EARTHQUAKE: THE CASE OF HOTEL MONTANA

Dominic Assimaki

Georgia Institute of Technology
Atlanta, GA 30332-0355
USA

Seokho Jeong

Georgia Institute of Technology
Atlanta, GA 30332-0355
USA

ABSTRACT

Unusually severe structural damage was reported during the 2010 M7.0 Haiti earthquake in the vicinity of Hotel Montana, located on top of a ridge in the district of Pétionville. Prompted by the observations, USGS seismic stations were deployed, and aftershock recordings indicated ground motion amplification on the top of the hill compared to adjacent stations on reference site conditions. The presence of topographic relief has been shown to significantly aggravate the consequences of strong ground motion during past events, and topographic amplification was therefore brought forward to justify the observations. To test this hypothesis, we conduct numerical simulations of the foothill ridge response on homogeneous halfspace, which quantitatively disagree, however, with the field data both in amplitude and in frequency. Conversely, our one-dimensional ground response analyses for the site conditions at the hilltop predict amplification in same frequency range as the field data, yet of significantly lower amplitude. We then conduct realistic simulations of the foothill ridge seismic response with soil layering, and qualitatively demonstrate that the recorded amplification can be attributed to a phenomenon here referred as *topography-modified site amplification*, which describes seismic waves trapped in the soft soil layers of the near surface and simultaneously subjected to site amplification, diffraction and scattering. Parametric investigations of the topography-soil amplification coupling effects are then conducted, and our results show that when accounting for a soil-bedrock interface at 100m depth, predictions are in excellent quantitative agreement with the observed motion

INTRODUCTION

The city of Port-au-Prince suffered widespread damage during the M7.0 Haiti earthquake of 12 January 2010, with an officially announced death toll of 230,000 (USGS, 2010), 97,294 residential structures destroyed, and 188,383 damaged beyond repair; the catastrophic consequences of the event were attributed to the proximity of epicenter and the poor construction quality of the residential structures. Site effects played a key role in the damage distribution (GEER, 2010), with sediment-induced amplification and ray focusing within the strong topographic relief being most likely phenomena explaining the macroseismic observations. In this paper, we focus on the case study of Hotel Montana, that was located along a foothill ridge in northern Pétionville and suffered extensive damage during the mainshock along with a number of adjacent residential structures. Due to the ground surface geometry at the site, the localized damage pattern was initially attributed to topography effects (Hough et al, 2010). In this paper, we follow up on this work by conducting numerical simulations that integrate Digital Elevation Maps (DEM) and Multi-Channel Analyses of Surface Waves (MASW) data collected at the sites by Cox et al (2011), and investigating the role of topography and ground surface response at the site by means of site-specific and parametric numerical simulations. Neither topography nor site amplification predictions alone sufficiently explain the ground motion amplification at the site estimated via aftershock recordings. Site-specific two-dimensional (2D) simulations of layered topographic features, however, do capture the frequency range of amplification, and when the effects of engineering bedrock impedance at 100m are accounted for, our simulations are found to be in excellent agreement with the recorded motions. We conclude therefore that the damage concentration at the foothill ridge most likely stemmed from *topography-modified site amplification*, namely coupling between topography and stratigraphy effects that refers to high frequency components trapped in the near surface soil layers of topographic features, and further amplified due to scattering and diffraction.

MACROSEISMIC OBSERVATIONS AND AFTERSHOCK RECORDINGS

Hough et al (2010) deployed eight portable K2 seismometers equipped with force-balance accelerometers and, at two stations, velocity transducers in order to explore the damage distribution within Port au Prince. Two of these instruments were deployed in late January, 2010 while the remaining six were deployed in early March. The location of the instruments is shown in Fig. 1, which also highlights the stations of interest in this study: station HHMT that was installed on the foothill ridge adjacent to Hotel Montana on medium stiff site conditions (Class C) with $V_{s30}=626\text{m/s}$, and station HCEA that was installed on competent (Class B) site conditions with $V_{s30}=1014\text{m/s}$ and was thus used as a reference station.

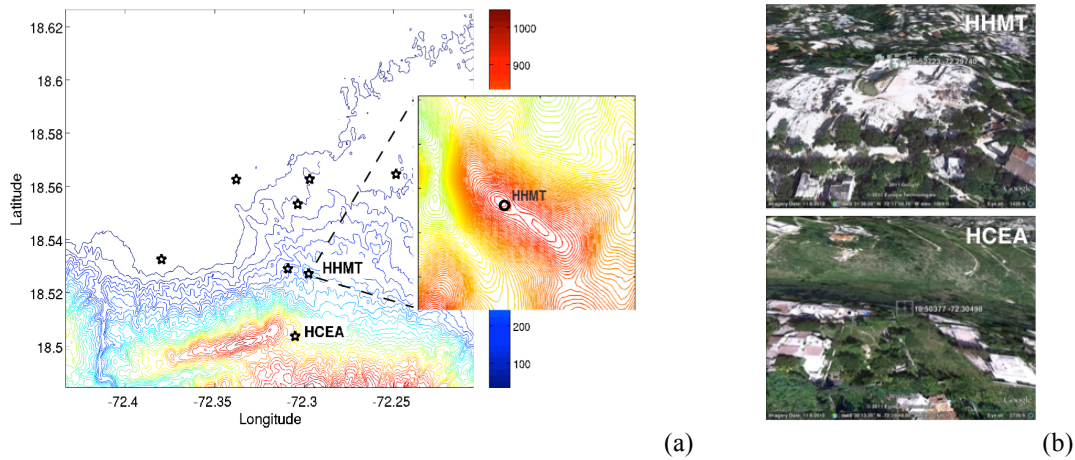


Fig. 1. (a) Contour map and instrumentation at Pétionville district: Station HHMT is located adjacent to Hotel Montana atop a foothill ridge (see detail on the right) and station HCEA is located on competent rock and was used as reference by Hough et al (2010); (b) Satellite image of the sites of interest (source: Google EarthTM)

A number of M3-4 aftershocks were recorded cleanly across the array with good signal-to-noise levels. We here present analysis of the largest aftershocks, namely six events with magnitudes between 3.7-4.4 (see Hough et al, 2010). Without processing, waveforms recorded at HHMT revealed significant amplification relative to the reference station HCEA in the frequency range [6-8] Hz as shown in Fig. 2. The ground surface topography at HHMT in conjunction with the localized damage pattern brought forward ray focusing in the topographic irregularity as the most likely phenomenon explaining the macroseismic observations. Note that the theoretical prediction of ground motion aggravation at HHMT using the infinite wedge model proposed by Sanchez-Sesma (1985) for a simplified geometry of the foothill ridge (internal angle 135°) yields a topographic amplification factor of 2.7 in the frequency range [0-7] Hz. The agreement between the theoretical predictions and ground motion recordings further supported the assumption of topography effects as the dominant factor in the observed damage concentration atop the ridge.

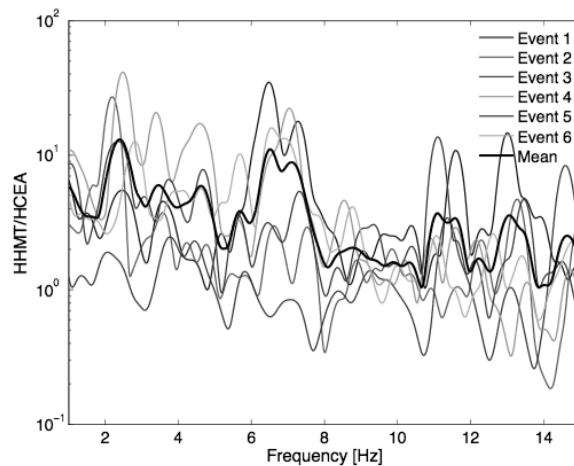


Fig. 2. Spectral amplification of aftershock recordings at HHMT relative to HCEA in the vicinity of 7Hz, attributed to topography amplification (modified from Hough et al, 2010).

Following up on the work by Hough et al (2010), we here conduct site-specific numerical simulations for the geometry and soil profile at station HHMT and compare our predictions with the recorded ground motion amplification. In the ensuing, we first present results of 1D site response analyses at HHMT and HCEA and illustrate the almost flat reference-type site amplification of the latter and the pronounced 7Hz first mode amplification of the former. Successively, we conduct 2D analyses of the geometry at HHMT and HCEA assuming homogeneous site conditions, and show that the observed spectral amplification cannot be explained by topography amplification alone. We finally combine the two models into realistic simulations of the foothill ridge seismic response, and qualitatively demonstrate that the observations are most likely the result of coupled topography-ground surface response effects, namely seismic wavelengths comparable to the thickness of soft surficial soil layers that are trapped in the near surface due to the stratigraphy of the site, and amplified in excess of one-dimensional (1D) site response due to diffraction and scattering. Parametric investigations of the geometry-soil coupling amplification are then conducted, and results show that when accounting for a soil-bedrock interface at 100m depth, predictions are in excellent quantitative agreement with the observed motion amplification.

ONE-DIMENSIONAL SITE RESPONSE ANALYSES

We first investigate the linear elastic response of sedimentary deposits at stations HHMT and HCEA. Following the mainshock, GEER (2010) sponsored an earthquake reconnaissance in the broader area of Port au Prince, and as part of this effort, Cox et al (2011) evaluated MASW shear wave velocity profiles at 36 sites. The soil profiles at the sites of interest are shown in Fig. 3(a), while the corresponding linear elastic frequency domain site response, evaluated by means of the Haskell-Thompson transfer matrix method, is shown in Fig. 3(b). As can be readily seen, the site response at station HHMT is characterized by pronounced first mode amplification at 7Hz, namely in the same frequency range as the observed ground motion amplification; the latter, however, was on the order of 10-20, approximately five times the predicted 1D amplification of 3-4. On the other hand, the stiff site conditions at HCEA render the site an excellent candidate for site amplification reference, as can be seen by the corresponding 1D site response of the profile in Fig. 3(b).

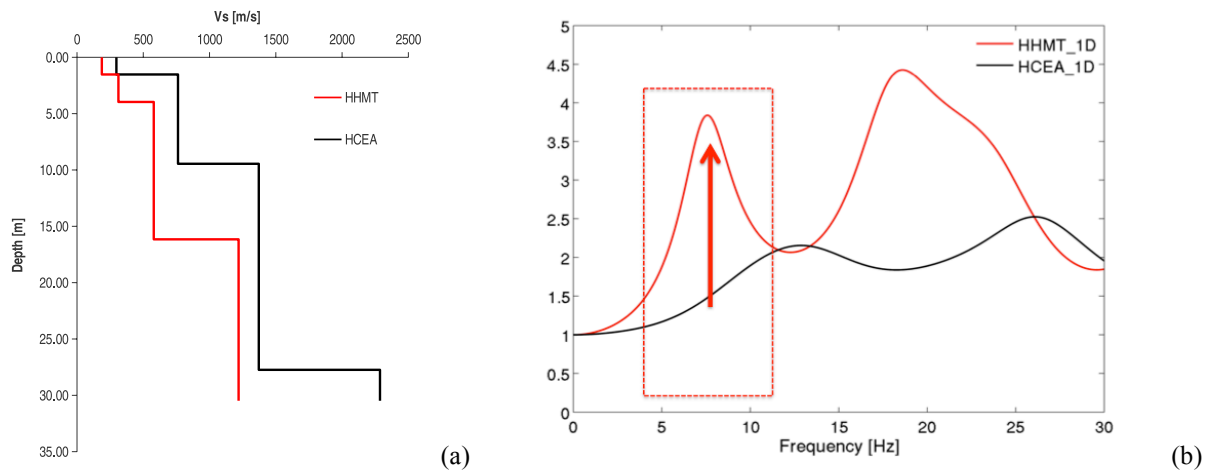


Fig. 3. (a) Shear wave velocity in the top 30m at stations HHMT and HCEA evaluated by means of multi-channel surface wave analysis, and (b) Haskell-Thompson transfer function at the two sites, revealing the HCEA site flat response in the frequency domain and the pronounced site amplification at 7Hz at site HHMT.

NUMERICAL SIMULATIONS OF TOPOGRAPHIC AMPLIFICATION

We next investigate the effects of surface topography on the aggravation of seismic motion relative to flat ground conditions. We first simulate the response of the topographic features at the locations of stations HHMT and HCEA by means of linear elastic two-dimensional analyses assuming homogeneous halfspace soil conditions. Successively, we integrate the effects of stratigraphy as continuous soil layers on the surface of the halfspace, and compute the coupled response of layered features with irregular ground surface geometry. The numerical models are shown in Fig. 4a and the simulations are conducted by means of the finite element computer code DYNFLOW (Prevost, 1995). The far field boundaries of the computational domain are located at adequate distance to approach 1D site response conditions and are constraint to respond as such, the ground motion is simulated as incident seismic pulse at the base of the models in the form of effective forces, and absorbing boundaries are implemented at the bottom of the model to represent the proper conditions of radiation damping. Details on our simulations of 2D topographic amplification by means of finite elements can be found in Assimaki et al (2005). The dimensions of the topographic features at HHMT and HCEA were

extracted from the Digital Elevation Map of the area shown in Fig. 1 (A. Yong, personal communication) while the shear wave velocity of the homogeneous halfspace is assigned as $V_s=2286\text{m/s}$, namely the bedrock velocity as measured at the reference station HCEA. It should be noted here that the ground surface topography at stations HHMT and HCEA is very similar, which in turn implies that the frequency response of the homogeneous irregular topographic features is also expected to be similar.

The features are subjected to an incident train of Ricker wavelets with central frequencies 0.5, 2.5, 5 and 10 Hz. The incident waveforms and corresponding Fourier Amplitude Spectra (FAS) are shown in Fig. 4b. Results are shown in Fig. 5a in the form of 3D FAS for site HHMT, depicting the amplification potential of the feature in the frequency domain as a function of space. The FAS on the vertices are successively compared in Fig. 5b, and as can be readily seen, the frequency response of the two features is almost identical in the frequency range where amplification was identified in the recorded ground motions. Given that the 1D ground response at HCEA as shown in Fig. 3 is approximately unity in the frequency range of interest [6-8] Hz, we here assume that the response of HCEA is approximately equal to the response of the homogeneous HHMT feature, and use the latter in the foregoing parametric analysis of topographic aggravation of ground motion by layered features.

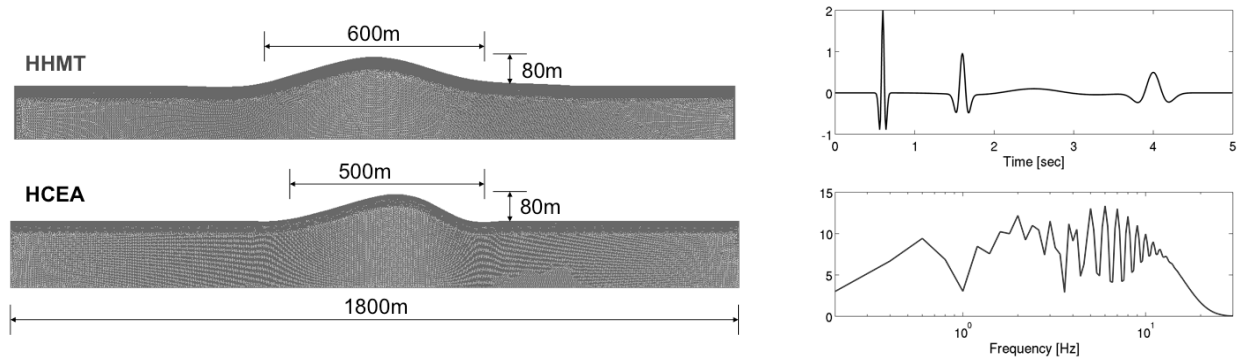


Fig. 4. (a) Two-dimensional finite element models of the topographic features on which stations HHMT and HCEA were installed, as extracted from the DEM of the Port au Prince region; (b) Incident idealized ground motion in numerical simulations in the form of a train of Ricker pulses: (top) waveform and (bottom)

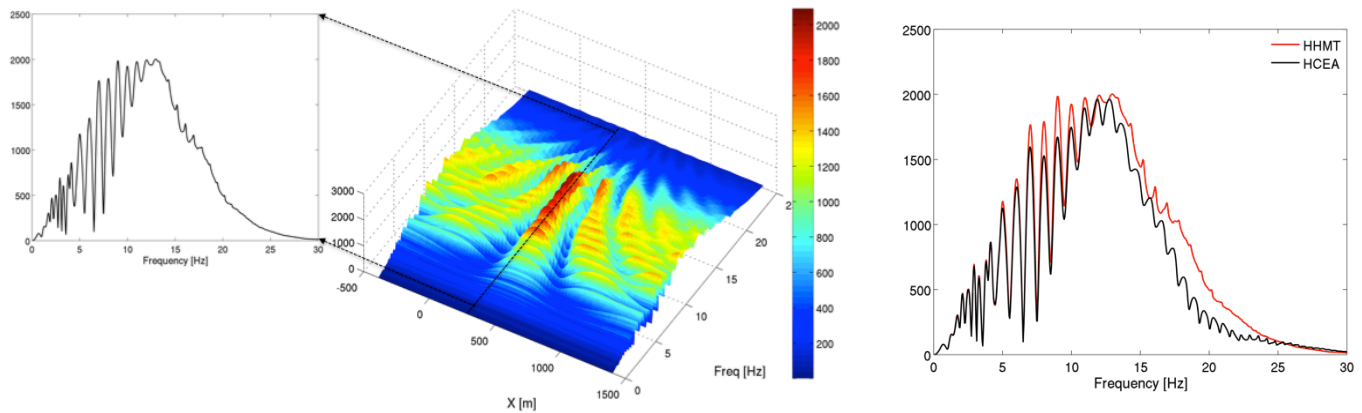


Fig. 5. Three-dimensional Fourier Amplitude Spectrum along the surface of the topographic feature of HHMT assuming homogeneous soil conditions, and comparison of the vertex FAS of HHMT and HCEA. Note that the homogeneous response of the two features is shown to be almost identical in the frequency range of ground motion recorded amplification.

Site-specific simulations of coupled stratigraphy-topography aggravation

Successively, the stratigraphy at station HHMT is combined with the two-dimensional cross section described above, and coupled soil-topography amplification simulations are conducted. In this case, a Ricker wavelet of central frequency 7Hz is selected as incident motion, anticipated to maximize amplification at the first resonant frequency of the soil profile. Note that, for the halfspace shear wave velocity of the simulations, a pulse with frequency 7Hz corresponds to wavelengths approximately equal to half the width of the topographic feature. As a result, the incident pulse is anticipated to give rise to topographic amplification phenomena as well.

Fig. 6 shows the horizontal acceleration synthetics computed along the surface of the model for the homogeneous ridge and the same feature with the soil profile at HHMT horizontally stratified parallel to the surface. The first arrivals, P waves and Rayleigh waves are clearly seen in the case of homogeneous ridge, whereas when the actual velocity profile is included in the model, the response is much more complex as a result of multiple reflections, refractions and mode conversions. Fig. 6 also depicts the normalized peak acceleration distributions along the surface of the homogeneous ridge and layered ridge subjected to the 7Hz central frequency Ricker pulse. In each case, the peak acceleration (horizontal and vertical) is normalized by the corresponding maximum value on flat ground, namely in the far field. Note that while the incident motion is purely horizontal, the ground surface response contains both horizontal and vertical components, the latter arising due to mode conversion from SV to SP waves and Rayleigh waves due to scattering of the arriving pulse on the irregular ground surface. Interestingly, while the homogeneous ridge shows 60% amplification of the horizontal ground motion relative to the far field, and 20% vertical (parasitic) acceleration, the layered ridge shows almost no topographic amplification, with the peak horizontal acceleration computed equal to the 1D layered site response; the mode conversion, however, in this case is more pronounced, with the vertical maximum acceleration estimated 35% the peak value on the surface of the far field layered medium. It should be noted, however, that the peak acceleration on the surface of the 1D layered structure is almost twice the amplitude of the homogeneous flat ground, and therefore, the parasitic acceleration in the case of the layered medium is 70% the corresponding peak acceleration on the far field of the homogeneous configuration.

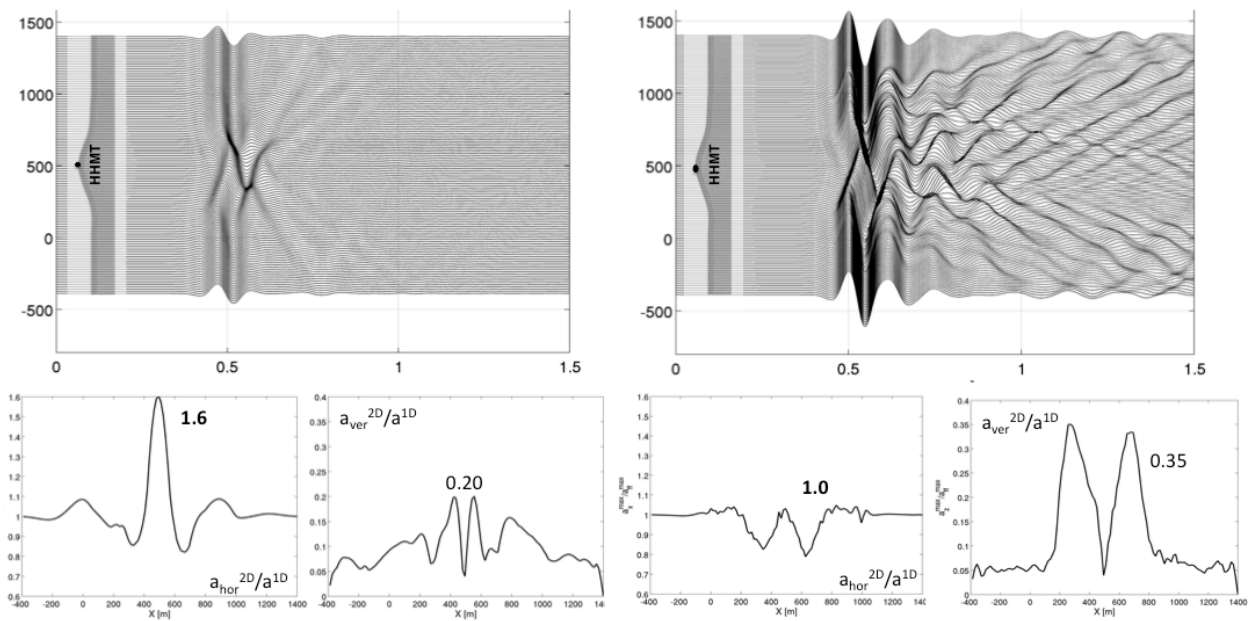


Fig. 6. Seismogram synthetics on the surface of the homogeneous (left) and layered (right) configurations, and spatial distribution of the maximum horizontal and vertical acceleration components for each case.

Results described above indicate that coupling between topography- and stratigraphy-induced amplification gives rise to complex phenomena not described by their superposition. More specifically, incident seismic waves in the near surface of irregular topographic features are trapped in the softer soil layers, and further amplified as a result of the impedance contrast, while simultaneously scattered and refracted due to the irregular surface geometry. To that end, Fig. 7 compares the 1D site response at HHMT to the acceleration spectral ratio of the layered HHMT ridge at the vertex over the homogeneous ridge response at the same location, the latter here approximating the response at the reference station, HCEA. As can be readily seen, the response of the stratified feature normalized by the response of the homogeneous feature is not equal to the 1D site response. Instead, coupling effects give rise to a so-called *topography-modified site response*, which differs from the far field 1D response by a frequency dependent factor $\alpha(\omega)$ as follows:

$$\frac{U_{\text{layered}}^{2D}}{U_{\text{homogeneous}}^{2D}} = U_{\text{layered}}^{1D} \cdot \alpha(\omega)$$

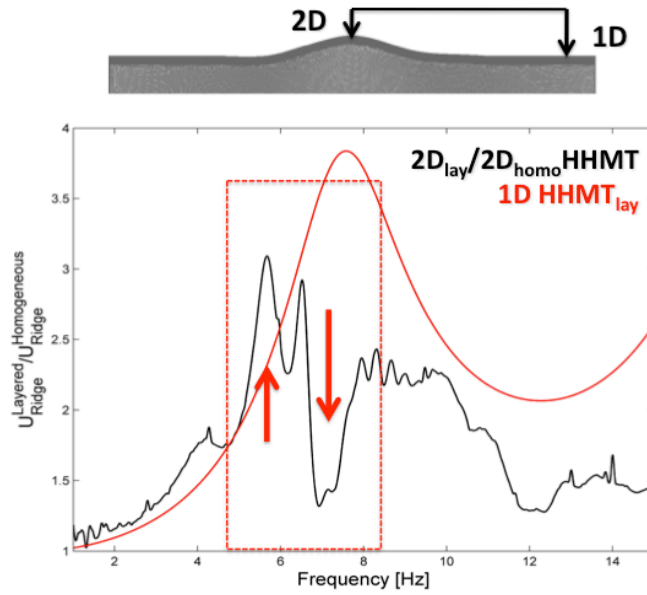


Fig. 7. Comparison of the 1D site response and the topography-modified site response at station HHMT.

Comparing the 1D response to the *topography-modified site response* at HHMT, we observe that the coupling effects reduce the overall amplification potential of the near surface stratigraphy at the profile first mode, while giving rise to a localized peak in the frequency range [6-8] Hz, namely in the range where amplification was observed in the recorded ground motions at Hotel Montana. Indeed, Fig. 8 compares the predicted *topography-modified site response* at HHMT to the mean frequency ratio of the recorded ground motions shown in Fig. 2, revealing qualitative agreement between the two in the frequency range [6-8] Hz. For comparison, the Fig. 8 also depicts the ratio of the predicted layered HHMT response to the predicted HCEA response accounting for the 1D layered structure at both features, and the 1D theoretical transfer function at HHMT. Results clearly illustrate that while neither topography nor sediment-induced amplification alone could explain the ground motion aggravation recorded at Hotel Montana, combined topography-stratigraphy amplification captures the frequency range of amplification. Quantitatively, however, numerical simulations and field observations show a clear discrepancy, differing in magnitude by a factor of three. In the following section, we identify the parameters most likely controlling the magnitude of ground motion amplification, and speculate the origin of discrepancy between theory and observations.

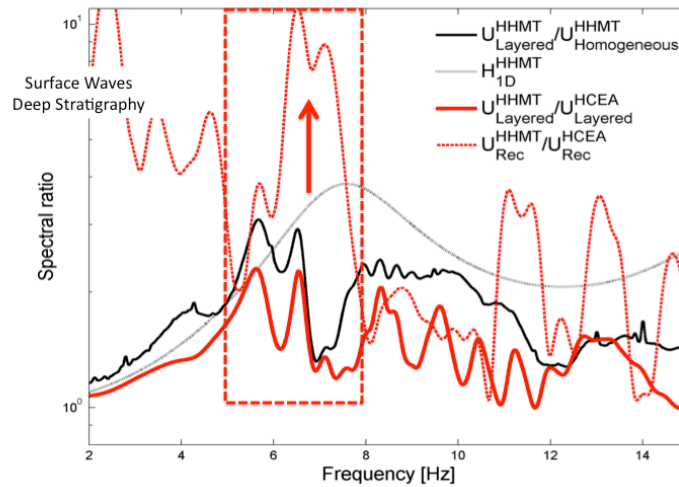


Fig. 8. Comparison between simulated and observed ground motion amplification at HHMT: the former is evaluated as the ratio of layered to homogeneous HHMT ridge at the vertex, layered HHMT to layered HCEA at the vertex, shown to be very similar due to the reference site conditions of the latter. The 1D transfer function at HHMT is also shown for comparison, to illustrate the concept of topography-modified site response.

PARAMETRIC INVESTIGATION OF COUPLED TOPOGRAPHY-SITE AMPLIFICATION

We have so far illustrated the concept of *topography-modified site response*, and qualitatively explained it as the trapping of seismic energy in the surficial soil layers, and their modification in amplitude, frequency and duration due to scattering and refraction within the convex ground surface geometry. Assimaki et al (2005) studied the coupling between site response and topographic amplification for a single slope configuration, and showed that the amplitude, frequency characteristics and spatial variability of topographic aggravation can be significantly altered by local site conditions. We here investigate the opposite effect, namely the altering of site amplification due to the presence of irregular ground surface geometry. For this purpose, we conduct a series of parametric analyses to identify the parameters affecting the magnitude, frequency content and spatial distribution of ground motion site amplification in the vicinity of convex features. More specifically we investigate the role of the thickness of the surficial layers normalized by the depth of the soil profile (t/h), the impedance contrast between the surface and underlying soil layers (α), and the impedance contrast between the soil layers and underlying bedrock (α_b). We here assume the location of bedrock at $h=100\text{m}$, a widespread geotechnical engineering assumption in absence of velocity data below 30m depth. For the purpose of the parametric investigation, the geometry and stratigraphy of the HHMT ridge are simplified as shown in Fig. 9(a).

Figure 9(b) compares the 3D FAS along the ground surface of the original and idealized HHMT ridge. The soil profile of the former corresponds to the MASW inversion shown in Fig. 3.a, while the latter is idealized by a two-layer formation, with the underlying soil layer velocity fixed to $V_{s2}=2286\text{m/s}$ (namely the halfspace velocity in the site-specific simulations), the thickness of the surficial soil layer $t=20\text{m}$, and the soil and soil-to-bedrock impedance contrasts equal to $\alpha=4$ and $\alpha_b=1$ respectively. Figure 9(c) compares the 2D to 1D amplification ratio at the vertex of the original and idealized HHMT layered ridge, as well as the spatial distribution of the peak horizontal and vertical acceleration normalized by the far-field peak acceleration for both cases. As can be readily seen, the idealized configuration approximates very closely the site-specific layered feature at HHMT, and will be heretofore used in the parametric investigation.

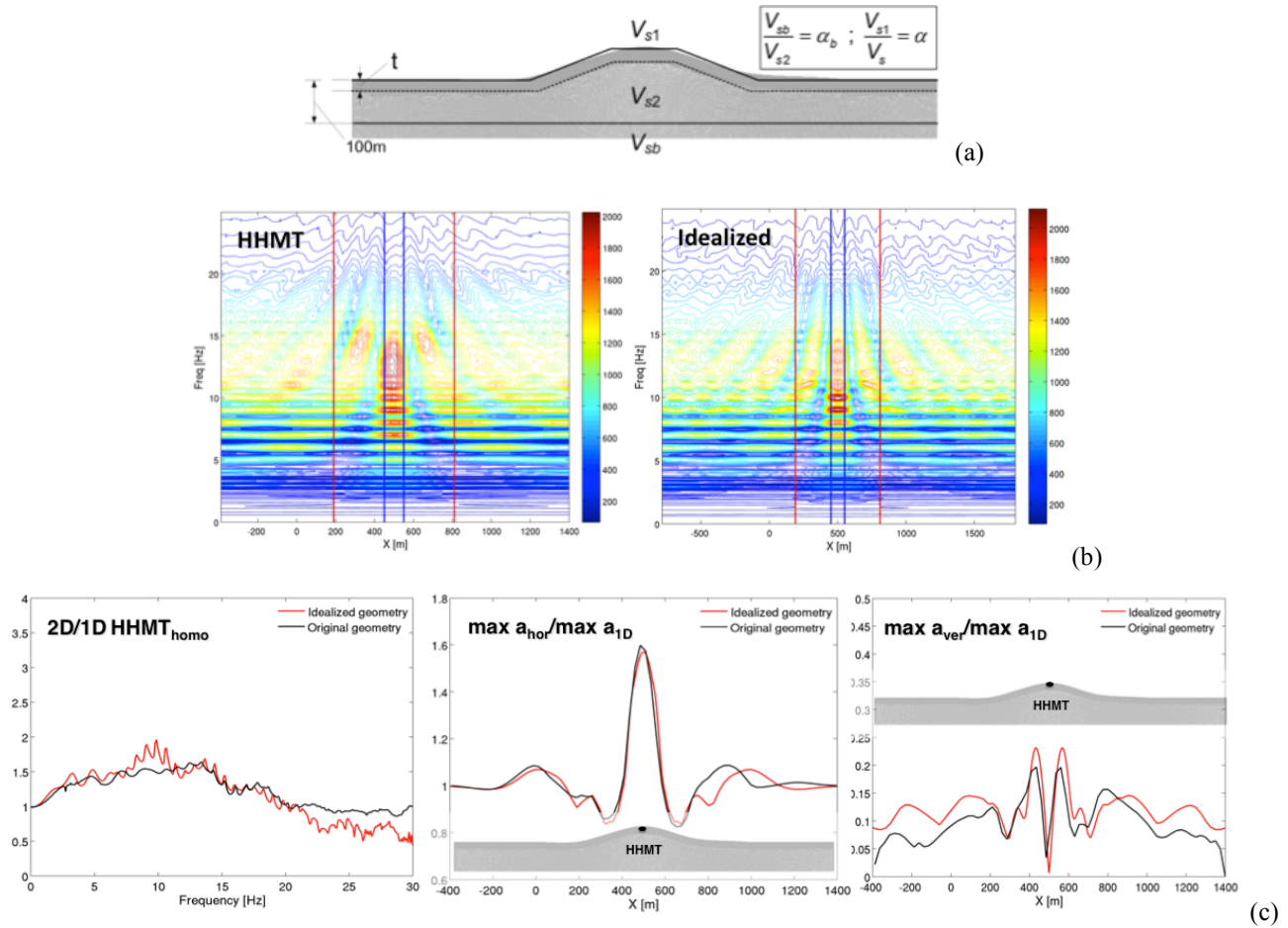


Fig. 9. Simplified geometry and stratigraphy at station HHMT used in the parametric investigation, and comparison of the idealized response to the site-specific configuration in space and frequency.

Results of the parametric analyses are summarized in Fig. 10. In each case, the response is compared to the original layered HHMT ridge amplification, as depicted in Fig. 7. The top row of Fig. 10 illustrates the effects of **soil-to-bedrock impedance** (α_b). Three cases are investigated here, namely $\alpha_b=1, 1.5$ and 2 , and as expected, the impedance contrast between soil and bedrock controls the amount of energy trapped in the soil formation above the bedrock: the stronger the contrast, the larger the amplification at the fundamental frequency of the near-surficial layers (here at 7Hz), while the amount of energy trapped in the near surface is in turn further aggravated by the presence of the irregular surface topography. The middle row of Fig. 10 depicts the effects of **surface soil stiffness** (here parameterized as $\alpha=V_{s2}/V_{s1}$). Three cases are investigated, namely $\alpha=2, 4$ and 6 , and can be seen, the surficial soil layer controls the fundamental (1D) frequency of the profile and in turn the frequency range of *topography-modified site response*. Given that $V_{s2}=2286\text{m/s}$ is fixed in our simulations, the higher the impedance contrast, the lower the resonant (1D) frequency of the soil profile and in turn the frequency range of *topography-modified site response*. Finally, the bottom row of Fig. 10 depicts the effects of surface soil layer thickness for three cases $t=10\text{m}, 20\text{m}$ and 40m . The thicker the soft sediments for impedance contrast $\alpha=4$ and bedrock soil impedance $\alpha_b=1$, the lower the 1D resonant frequency of the soil profile and thus the frequency range of *topographic aggravation of seismic motion*. Parametric analyses show that the amplitude discrepancy between predictions and observations is most likely originating from incomplete information of the local soil conditions at HHMT (30m deep profile available), while the presence of a soil-bedrock interface at the base of the profile (here 100m depth) yields ground motion amplification that quantitatively agrees with the recorded spectral ratios at Hotel Montana.

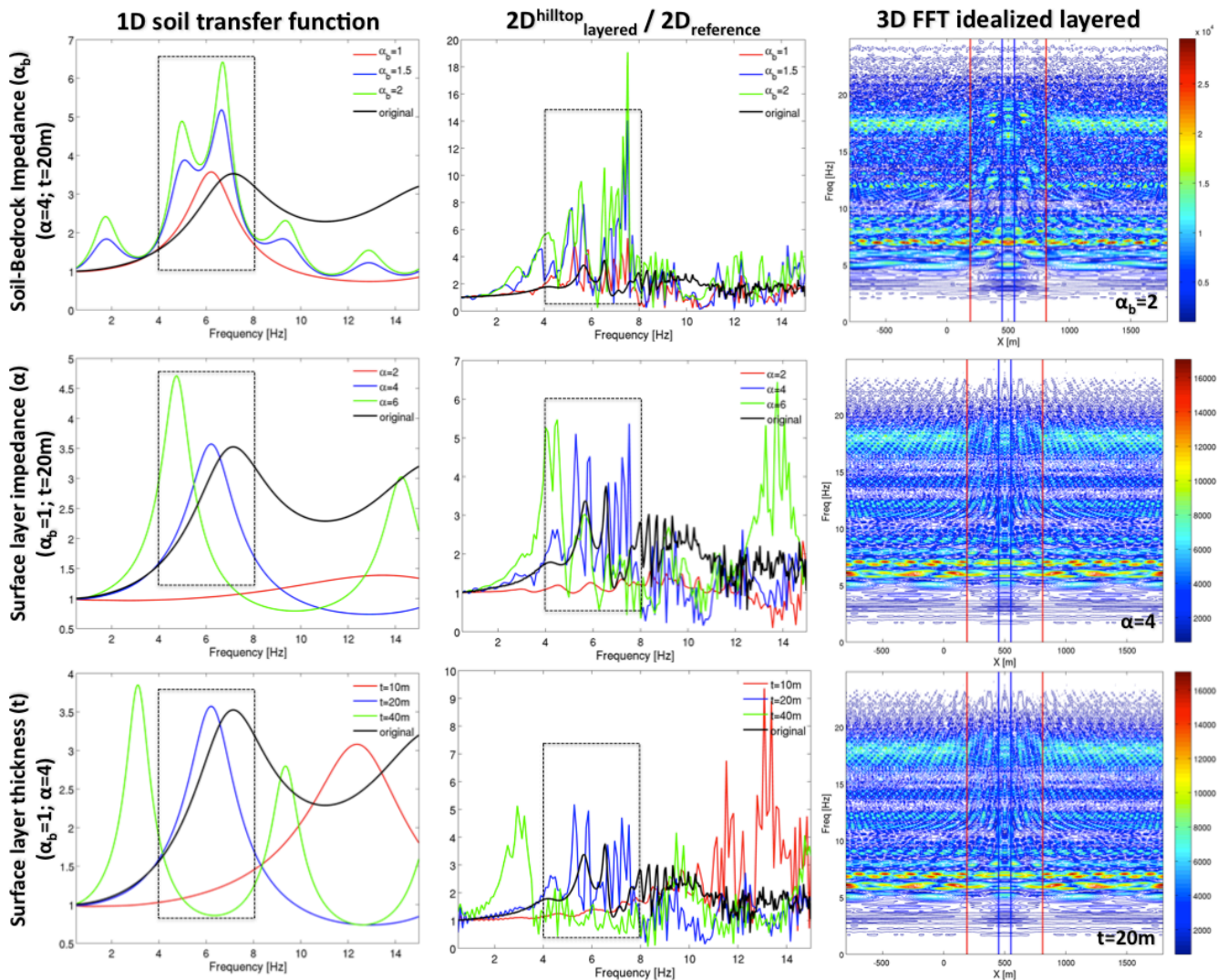


Fig. 10. Parametric investigation of topography-modified site response: Effects of soil-to-bedrock impedance (top), surface to underlying soil layer impedance (middle), and surface soil layer thickness (bottom).

DISCUSSION-CONCLUSIONS

Following up on the work by Hough et al (2010), we conducted site-specific analyses of coupled topography-stratigraphy effects at the hilltop ridge of Hotel Montana. Our simulations revealed that the observed ground motion amplification at station HHMT relative to the reference station HCEA on competent rock is most likely a result of *topography-modified site response*. Observations and site-specific simulations were found to be in excellent qualitative agreement, yet quantitatively, the predicted amplification in the frequency range [6-8] Hz was found to underestimate the field recordings by a factor of three. We next investigated the parameters controlling the amplitude and frequency content of topography-modified site response, and identified the thickness of sediments, the surface layer stiffness and soil-bedrock impedance as the dominant parameters controlling the phenomenon. The soil to bedrock impedance was shown to affect the amplitude of surface ground motion in the resonant frequency of the surface sediments, and for a contrast equal to $\alpha_b = 2$, the predicted ground motion amplification quantitatively compares with the observations in frequency and amplitude as shown in Fig. 11. We therefore conclude that the ground motion observations at Hotel Montana and the damage concentration at the hilltop was governed by soil amplification effects, manifesting in the frequency range of 1D site response [7Hz] and modified due to scattering and refraction on the irregular ground surface. Soil characterization was available only at the top 30m of the HHMT site, and most likely, the presence of a deeper soil-bedrock interface further aggravated the amplification of seismic waves in the near surface. Our study shows that coupling between topography and site response effects gives rise to complex wave propagation patterns in excess of the two phenomena alone, and a more detailed parametric investigation of the phenomenon for generic topographic features and soil profiles is currently in progress by the authors.

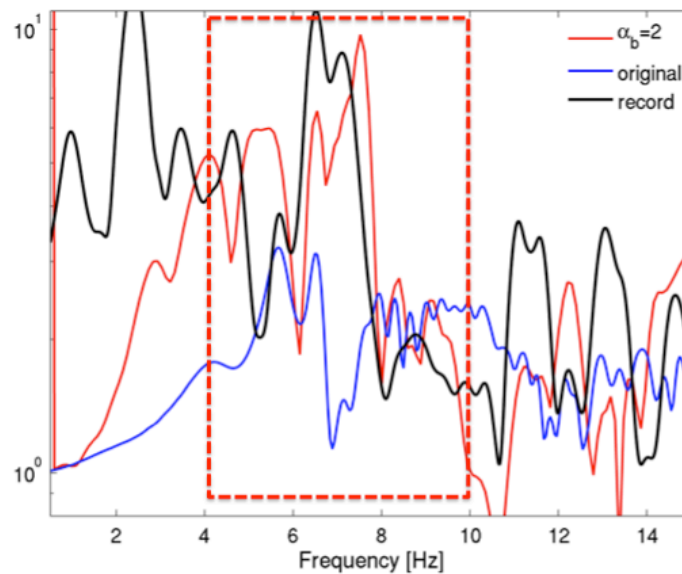


Fig. 11. Comparison between observed and predicted ground motion amplification, defined as the ratio of the ground motion predicted at HHMT over HCEA stations; Predictions include the original topographic features at HHTM and HCEA with the stratigraphy available (top 30m) from site investigation, as well as the result of parametric analyses where a soil-bedrock interface is assumed at 100m depth with impedance contrast $\alpha_b = 2$. The latter is in excellent agreement with the observations.

ACKNOWLEDGEMENTS

The authors would like to thank Dr. Susan E. Hough and Alan Yong from the U.S. Geological Survey, Pasadena, CA and Dr. Brady Cox from the Civil Engineering Department at the University of Arkansas for providing the seismic ground motion, digital elevation maps, and soil profile data to us, and engaging in discussions that helped us gain insight during the preparation of this paper. Their help and support is hereby acknowledged.

REFERENCES

Assimaki D., Gazetas G. and Kausel E. [2005]. Effects of local soil conditions on the topographic aggravation of seismic motion: Parametric investigation and recorded field evidence from the 1999 Athens Earthquake, *Bull. Seism. Soc. Am.*, 95(3), 1059-1089

Cox, B.R., Bachhuber, J., Rathje, E., Wood, C.M., Dulberg, R., Kottke, A., Green, R., Olson, S. [2011]. Shear Wave Velocity- and Geology-based Seismic Microzonation of Port-au-Prince, Haiti, Earthquake Spectra, (accepted for publication)

GEER [2010]. Geotechnical Engineering Reconnaissance of the 2010 Haiti Earthquake, Report of the National Science Foundation-Sponsored Geoenvironmental Extreme Events Reconnaissance Team (http://www.geerassociation.org/GEER_Post%20EQ%20Reports/Haiti_2010/Cover_Haiti10.html)

Haskell, N. A. [1953]. The dispersion of surface waves on multilayered media, Bull. Seism. Soc. Am., 62, 1231–1258

Hough, S. E. et al. [2010]. Localized damage caused by topographic amplification during the 2010 M 7.0 Haiti Earthquake, Nature Geoscience, 3, 778–782.

Prévost, J. H. [1981]. DYNAFLOW: A nonlinear transient finite element analysis programme, Dept. of Civil Engineering, Princeton University

Sanchez-Sesma, F. J. [1985]. Diffraction of elastic SH waves by wedges, Bull. Seism. Soc. Am. 75, 1435-1446

Thompson, W. T. [1950]. Transmission of elastic waves through a stratified soil medium, J. Appl. Phys., 21, 89–93.

USGS [2010]. <http://earthquake.usgs.gov/earthquakes/eqinthenews/2010/us2010rja6/>

For additional information or clarification, please contact:

Sandra Seale
Earth Research Institute
University of California Santa Barbara
Santa Barbara, CA 93106 USA
Phone: 805-893-8543
FAX: 805-893-2578
E-mail: esg4@eri.ucsb.edu